pubs.acs.org/IC

Ligand Control of Supramolecular Chloride Photorelease

Michael D. Turlington, Ludovic Troian-Gautier, Renato N. Sampaio, Evan E. Beauvilliers, and Gerald J. Meyer*®

Department of Chemistry, University of North Carolina at Chapel Hill, Murray Hall 2202B, Chapel Hill, North Carolina 27599-3290, United States

Supporting Information

ABSTRACT: Supramolecular assembly is shown to provide control over excited-state chloride release. Two dicationic chromophores were designed with a ligand that recognizes halide ions in CH₂Cl₂ and a luminescent excited state whose dipole was directed toward, 12+, or away, 22+, from an associated chloride ion. The dipole orientation had little influence on the ground-state equilibrium constant, $K_{\rm eq} \sim 4 \times 10^6 \, {\rm M}^{-1}$, but induced a profound change in the excited-state equilibrium. Light excitation of [12+,Cl-]+ resulted in time-dependent shifts in the photoluminescence spectra with the appearance of biexponential kinetics consistent with the photorelease of Cl-. Remarkably, the excited-state equilibrium constant was lowered by a factor of 20 and resulted in nearly 45% dissociation of

chloride. In contrast, light excitation of $[2^{2+},Cl^{-}]^{+}$ revealed a 45-fold increase in the excited-state equilibrium constant. The data show that rational design and supramolecular assembly enables the detection and photorelease of chloride ions with the potential for future applications in biology and chemistry.

INTRODUCTION

The important role halide ions play in chemistry and biology has inspired research into halide sensing. 1-10 The contactless nature of luminescent sensors is particularly attractive for fundamental study and has led to the rational design of chromophores that specifically recognize halides. Amides and functional groups capable of hydrogen bonding have, in particular, been shown to recognize halide ions present in solution. 11-13 In spite of the remarkable advances in halide sensing, receptors that reversibly bind and then promote controlled halide release have not been developed.

To date, halide release is limited to transition-metal complexes that utilize reactive excited states for photoaquation of a halide ligand, as in nonluminescent PtIV complexes. 14 For example, ultraviolet or d-d excitation of [PtBr₆]²⁻ in water results in Br release with a quantum yield (ϕ) of 0.4. 15–18 Similarly, illumination of [PtCl₆]²⁻ also gave the aquation product and free Cl⁻, but the mechanism was complicated by additional redox chemistry. ^{19,20} Seminal work in the 1970s on the thermal and photochemical release of ligands from CrIII complexes, such as [Cr(NH₃)₅Cl]²⁺, revealed preferential photoaquation reactions that differed from the thermal aquation. 21 For [Cr(NH₃)₅Cl]²⁺, photoaquation primarily causes the release of NH₃ (ϕ = 0.35) and only minimal Cl⁻ release ($\phi = 2 \times 10^{-4}$). Adamson's empirical rules for these reactions have been used to design transition-metal complexes that preferentially release halide from the metal coordination sphere upon illumination.²² For example, trans-[Cr(en)₂Cl₂]⁺ undergoes photoaquation of a chloride ligand with a ϕ from 0.32 to 0.35 in acidic aqueous solution. 23 The corresponding cis- and trans-[Co(en)2Cl2]+ complexes show similar photochemistry but with a much lower efficiency (ϕ from 10⁻³ to 10⁻⁴).^{24,25} Significantly, this ligand-field photochemistry is irreversible and therefore differs from this report.

Herein two chromophores were designed that exploit receptor properties for supramolecular association with halide and excited-state characteristics relevant for reversible halide release. The chromophores shown in Figure 1 include a common ligand for halide coordination and a net charge of 2+ for electrostatic attraction. The second important design element is the orientation of the excited-state dipole. In chromophore [Ru(dtb)₂(daea)]²⁺ (1²⁺), the metal-to-ligand charge-transfer (MLCT) excited-state dipole is directed toward the halide binding site, while for $[Ru(btfmb)_2(daea)]^{2+}(2^{2+})$, it



Figure 1. Proposed supramolecular assembly structure of $\mathbf{1}^{2+}$ or $\mathbf{2}^{2+}$ and chloride (green sphere). The dipole orientation is indicated for the excited states of 1^{2+} (pink) and 2^{2+} (red).

Received: March 6, 2018 Published: April 25, 2018

is directed away. This orientation had no significant influence on the ground-state halide association but did have a profound influence on the photoluminescence (PL) of both excited states. In the case of $\mathbf{1}^{2+}$, the excited-state equilibrium constant for chloride association was 20 times smaller than that of the ground state, and light excitation of the adduct $[\mathbf{1}^{2+},\mathbf{Cl}^{-}]^+$ resulted in photorelease of the chloride ion. In the case of $\mathbf{2}^{2+}$, no evidence for chloride release was observed, but rather a 45-fold increase in the equilibrium constant was determined through the Förster cycle. Hence, supramolecular assembly can be utilized to recognize and photorelease chloride, behavior that may one day enable additional applications such as quantifying halide transport across artificial and natural membranes relevant to seawater desalination and cystic fibrosis related diseases. $^{26-28}$

EXPERIMENTAL SECTION

Materials. Dichloromethane (CH2Cl2; Burdick and Jackson, 99.98%) was used as received. Argon and nitrogen gas (Airgas, 99.998%) were passed through a Drierite drying tube before use. Ammonium hexafluorophosphate (NH₄PF₆; Sigma-Aldrich, ≥ 98%), tetrabutylammonium chloride (TBACl; Sigma-Aldrich, purum ≥97%), tetrabutylammonium perchlorate (TBAPF₆; Sigma-Aldrich, for electrochemical analysis, ≥ 98%), sodium tetrakis[3,5-bis-(trifluoromethyl)phenyl]borate [NaB(ArF)₄; ArkPharm, 97%], and ruthenium trichloride hydrate (Oakwood Chemicals) were used as received. NMR solvents were purchased from Cambridge Isotope Laboratories, Inc. Ru(dtb)₂Cl₂·2H₂O and Ru(btfmb)₂Cl₂ were synthesized according to a literature procedure. 29,30 chemicals were obtained from commercial distributors with a minimum purity of 98% and used as received. All solutions were purged with argon for at least 30 min before all electrochemical, titration, and transient PL experiments.

NMR. Characteristic NMR spectra were obtained at room temperature on a Bruker Avance III 400 or 500 MHz spectrometer. Solvent residual peaks were used as internal standards for ^1H [δ 2.50 for dimethyl sulfoxide (DMSO), δ 1.94 for CD₃CN, and δ 5.32 for CD₂Cl₂] and ^{13}C (δ 39.52 for DMSO) chemical shift referencing. NMR spectra were processed using *MNOVA*.

Mass Spectrometry. Samples were analyzed with a hybrid LTQ FT (ICR 7T; ThermoFisher, Bremen, Germany) mass spectrometer.

UV-Vis Absorption. UV-vis absorption spectra were recorded on a Varian Cary 60 UV-vis spectrophotometer with a resolution of 1 nm.

Steady-State PL. Steady-state PL spectra were recorded on a Horiba Fluorolog 3 fluorimeter and corrected by calibration with a standard tungsten—halogen lamp. Samples were excited at 450 nm. The intensity was integrated for 0.1 s at 1 nm resolution and averaged over three scans. The PL quantum yields were measured by an optically dilute method using $[Ru(bpy)_3][PF_6]_2$ in acetonitrile ($\Phi = 0.062$) as a quantum yield standard.

Time-Resolved PL. Time-resolved PL data were acquired on a nitrogen dye laser with excitation centered at 500 nm. Pulsed-light excitation was achieved with a Photon Technology International (PTI) GL-301 dye laser that was pumped by a PTI GL-3300 nitrogen laser. PL was detected by a Hamamatsu R928 photomultiplier tube optically coupled to a ScienceTech model 9010 monochromator terminated into a LeCroy Waverunner LT322 oscilloscope. Decays were monitored at the PL maximum and averaged over 90 scans. Nonradiative and radiative rate constants were calculated from the quantum yields, $\Phi = k_{\rm r}/(k_{\rm r} + k_{\rm nr})$, and lifetimes, $\tau = 1/(k_{\rm r} + k_{\rm nr})$.

Transient PL. Transient PL data were obtained on the nitrogen dye laser described above. Excited-state decay traces were obtained every 10 nm from 560 to 770 nm and averaged over 60 scans. The amplitude of each PL decay after a specific time delay from the laser pulse (45 ns to 3 μ s at given intervals) was plotted versus the wavelength, and the data were normalized to give the transient PL spectra shown in Figure 3.

Excited-State Equilibrium. The solutions to the rates in eqs 1 and 2 are described elsewhere. $^{32-34}$ Because PL does not report on the concentrations of the excited-state complexes $\mathbf{1}^{2+}$ and $[\mathbf{1}^{2+},\mathbf{Cl}^-]^+$, the constants a and b were introduced for the appropriate conversion. Values for k_1 and k_2 were obtained in the absence or presence of 200 equiv of chloride. At these boundary conditions, the time-resolved PL traces displayed first-order kinetics, indicating that only one emissive species was present.

Electrochemistry. Square-wave voltammetry was performed with a BASi Epsilon potentiostat in a standard three-electrode cell in a CH₂Cl₂ electrolyte. The cells consisted of a platinum working electrode and a platinum mesh as an auxiliary electrode. A nonaqueous silver/silver chloride electrode (Pine) was used as a reference electrode that was referenced to an internal ferrocene (724 mV vs NHE).³⁶ or decamethylferrocene (Me₁₀Fc) standard (250 mV vs NHE).³⁶ The experiments were performed with 1.0 mM ruthenium solutions in 0.1 M TBACIO.

Halide Titrations. UV–vis, PL, and time-resolved measurements were performed in CH₂Cl₂ using approximately 10 μM solutions of 1^{2+} and 2^{2+} . Titration measurements were performed for each of the spectroscopies using TBACl through additions of 0.25 equiv. Throughout all titrations, the concentration of ruthenium complexes remained unchanged. In order to do so, a stock solution of each complex with an absorbance of ~0.1 at 450 nm in the desired solvent was prepared. The stock solution was transferred into a spectrophotometric quartz cuvette (5 mL). A titration solution was then prepared with 25 mL of the complex's stock solution. TBACl was added to the stock solution to obtain the desired concentration of halide. These solutions were then titrated to the quartz cuvette.

The 1 H NMR titrations were performed using a Bruker Avance III 500 MHz spectrometer equipped with a broad-band inverse probe with a 1 mM ruthenium complex in 600 μ L of a deuterated solvent, and 0.20 equiv of TBACl was added in 10 μ L additions. The ruthenium concentration was kept unchanged throughout by the preparation of a titration solution that contained both the desired complex and the desired halide. Each spectrum was averaged over 16 scans.

Data analysis for all experiments was performed using *OriginLab*, version 9.0. Data fitting was performed using a Levenberg—Marquardt iteration method. Benesi—Hildebrand-type analysis was performed in *Mathematica*, version 10.

Synthesis. *daea.* To 1.0 g (3.7 mmol) of 4,4′-dimethylester-2,2′-bipyridine in 20 mL of methanol was added 5 mL (5.15 g, 49 mmol) of 2-[(2-aminoethyl)amino]ethanolamine. The mixture was refluxed for 4 h. After cooling, ~25 mL of acetone was added to the resulting mixture, which was then filtered on a sintered-glass frit. The precipitate was washed with a copious amount of acetone and dried in an evacuated oven overnight at 150 °C to yield the title compound as a white powder (1.1 g, 72%). ¹H NMR (500 MHz, DMSO- d_6): δ 8.93 (t, J = 5.6 Hz, 2H), 8.86 (d, J = 5.0 Hz, 2H), 8.79 (d, J = 1.6 Hz, 2H), 7.85 (dd, J = 5.0 and 1.7 Hz, 2H), 4.48 (t, J = 5.3 Hz, 2H), 3.44 (q, J = 5.5 Hz, 4H), 3.38 (q, J = 6.3 Hz, 4H), 2.72 (t, J = 6.5 Hz, 4H), 2.60 (t, J = 5.8 Hz, 4H). ¹³C NMR (126 MHz, DMSO- d_6): δ 164.63, 155.51, 150.03, 142.99, 121.99, 118.25, 60.47, 51.51, 48.39, 39.52.

 $[Ru(dtb)_2(daea)](PF_6)_2$ (1²⁺). To a 10 mL glass microwave vial was added Ru(dtb)₂Cl₂·2H₂O (100 mg, 0.14 mmol), daea (70 mg, 0.17 mmol), and 5 mL of water containing 3 drops of concentrated HCl. The mixture was heated under microwave radiation by an Anton Paar Monowave 300 at 150 °C for 10 min. The mixture was brought to room temperature and filtered on a sintered-glass frit. The filtrate was then neutralized with sodium bicarbonate and stirred for 15 min. A saturated aqueous NH₄PF₆ solution was then added, and the formed precipitate was filtered on a sintered-glass frit and washed with water. The precipitate was then dried under vacuum to give the desired product (127 mg, 67%). 1 H NMR (CD₃CN, 500 MHz): δ 9.02 (s, 2H), 8.48 (dd, 4H), 7.84 (d, 2H), 7.73 (d, 2H), 7.55 (d, 4H), 7.42 (dd, 2H), 7.35 (dd, 2H), 3.56 (t, 4H), 3.51 (m, 4H), 2.85 (t, 4H), 2.73 (t, 4H), 1.41 (s, 18H), 1.39 (s, 18H). HRMS (ESI-MS). Calcd for $C_{56}H_{76}N_{10}O_4P_2Ru_1F_{12}Na_1$ ([M + Na]⁺): m/z 1367.28. Found: m/z1367.43.

[Ru(btfmb)₂(daea)](PF₆)₂ (2²⁺). To a 50 mL round-bottomed flask was added Ru(btfmb)₂Cl₂ (200 mg, 0.26 mmol), daea (110 mg, 0.26 mmol), AgNO₃ (90 mg, 0.53 mmol), and 16 mL of water/ethanol (1:1, v/v). The mixture was purged with N₂ for 30 min and then refluxed for 5 h under N₂. After cooling, the mixture was filtered and the solvent was removed from the filtrate, giving a red solid. The solid was dissolved in minimal water (about 3 mL) and precipitated by the addition of a saturated aqueous NH₄PF₆ solution. The solid was collected by filtration, washed with excess water, and dried under vacuum. The title compound was finally obtained as a dark-red solid (128 mg, 35%). ¹H NMR (CD₃CN, 500 MHz): δ 9.02 (s, 2H), 8.96 (s, 4H), 8.18 (s, 2H), 7.97 (dd, 4H), 7.87 (d, 2H), 7.74 (m, 6H), 3.72 (m, 8H), 3.24 (t, 4H), 3.11 (t, 4H). HRMS (ESI-MS). Calcd for C₄₄H₄₀F₁₂N₁₀O₄Ru ([M]²⁺): m/z 551.10429. Found: m/z 551.1049.

This complex as isolated was not soluble in CH₂Cl₂, which prevented its characterization in that solvent. To enhance the solubility in CH₂Cl₂, ion metathesis to the B(ArF)₄ salt was performed following a previously published procedure.^{37,38} Briefly, a 95% yield of [Ru(dtfmb)₂(daea)](NO₃)₂ was assumed for the solid obtained from the reaction mixture after evaporation, as described above. This solid was dissolved in minimal water (5 mL), and NaB(ArF)₄ (200 mg, 2 equiv relative to the predicted ruthenium yield) in methanol (3 mL) was added, causing a precipitate to form. The solid was collected by filtration and washed with excess water. All subsequent experiments were performed using the B(ArF)₄ salt of the complex.

■ RESULTS AND DISCUSSION

The diamide ligand for halide recognition shown in Figure 1 is abbreviated as daea and was synthesized by refluxing 4,4'dimethylester-2,2'-bipyridine in the presence of a large excess of 2-[(2-aminoethyl)amino]ethanol in methanol for 4 h. Microwave irradiation of this ligand with Ru(dtb)₂Cl₂ (dtb = 4,4'-di-tert-butyl-2,2'-bipyridine) in water gave complex 1^{2+} , which was further isolated as the ${\rm PF_6}^-$ salt. Complex 2^{2+} was obtained by refluxing the daea ligand with Ru(btfmb)₂Cl₂ [btfmb = 4,4'-bis(trifluoromethyl)-2,2'-bipyridine] and silver nitrate in water/methanol (1:1) for 5 h. Ion metathesis was finally performed to obtain 22+ as a B(ArF)4 salt (Figures S1-S6). All subsequent experiments were performed in CH₂Cl₂. Square-wave voltammetry was used to determine the RuIII/II and ligand-based reduction potentials. Because of the electronwithdrawing btfmb ligand, the Ru^{III/II} potential of 2²⁺ was found to be 300 mV more positive than that of 1^{2+} , and the first ligand-based reduction potentials were -880 and -470 mV versus NHE for 1^{2+} and 2^{2+} , respectively (Figure S7).

The use of ¹H NMR spectroscopy provided insight into the coordination environment of the chloride ions. Anions are known to affect the local magnetic environment of neighboring nuclei, such that the chemical shift can report on the specific location of a halide ion. 39-42 Tetrabutylammonium chloride titrations into solutions of 1^{2+} and 2^{2+} showed that the 3,3' protons on the daea ligand, as well as the amide protons, displayed significant downfield shifts, while the other resonances remained unchanged (Figures S8 and S9). These downfield shifts saturated after 1 equiv of chloride was added, pointing toward a one-to-one stoichiometry. The ¹H NMR data indicate that a single chloride ion binds to the two amide groups and the acidic H atoms of the bipyridine ligand, which elongates the C-H and N-H bonds and thereby reduces the electron density at these protons, causing downfield shifts of the signals. 40 This behavior has been observed for halide selfassembly to related chromophores. 40,41,43

The UV-vis absorption spectra of 1^{2+} and 2^{2+} in CH_2Cl_2 were typical of ruthenium polypyridyl complexes (Figure 2).

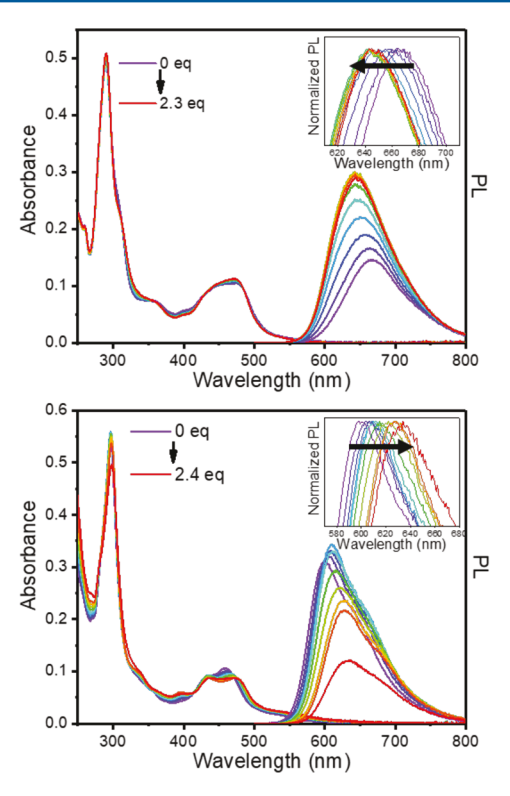


Figure 2. Absorption and PL changes of 1^{2+} (top) and 2^{2+} (bottom) upon titration of chloride from 0 to 2.3/2.4 equiv in CH_2Cl_2 . Insets show the normalized PL shifts upon titration of chloride.

The broad absorption from 400 to 500 nm was ascribed to metal-to-ligand charge-transfer (MLCT) transitions, while the features at or below 300 nm were assigned to ligand-centered π -to- π * transitions. Upon absorption of visible light, both complexes displayed room temperature PL with maxima at 665 and 600 nm for 1^{2+} and 2^{2+} , respectively.

Chloride titrations into solutions of 1^{2+} or 2^{2+} induced significant spectral shifts in the MLCT absorption band that saturated after about 1 equiv, consistent with strong ion pairing of chloride (Figure 2). A Benesi-Hildebrand analysis revealed a large equilibrium constant of $3.9 \times 10^6 \text{ M}^{-1}$ for 1^{2+} (Figure S10). 40,44 An accurate K_{eq} determination for 2^{2+} was hindered by precipitation of the chromophore and potential ligand substitution at high chloride concentrations; however, the absorption changes over the chloride concentration allowed were in good agreement with that of 1^{2+} from which a value of $4 \times 10^6 \text{ M}^{-1}$ was estimated (Figure S11). Supramolecular assembly was also observed with Br and I, but excited-state reactivity complicated further analysis with these halides. Additionally, experiments in more polar solvents such as CH₃CN revealed ground-state equilibrium constants that were systematically 1–2 orders of magnitude smaller $(6.7 \times 10^4 \, \mathrm{M}^{-1})$ for 1²⁺ with Cl⁻) than those observed in CH₂Cl₂, which has also been observed for related compounds.⁴¹

The steady-state PL spectra also shifted in energy as chloride was titrated into the solution. In the case of 1^{2+*}, the PL maximum blue-shifted and increased in intensity with increased Cl⁻ concentrations to about 1 equiv. Previous reports have attributed related excited-state interactions to halide-induced planarization of the two pyridyl rings. ^{30,45} For 2^{2+*}, the excited state was localized on the **btfmb** ancillary ligand (as discussed below), and a red shift in the PL was observed upon chloride titration. The red shift was accompanied by a change in the PL

intensity, but precipitation and potential ligand substitution at higher chloride concentrations precluded a more detailed analysis. Indeed, precipitation in these experiments was observed as a baseline shift in the delta absorbance spectrum (Figure S11), which was also concurrent with a moderate growth at 570 nm that could correspond to ligand substitution. 43,46 Both of these results contribute to the decrease in PL intensity.

The fact that the supramolecular assembly of chloride ions caused a PL blue shift for 12+* and a PL red shift for 22+* can be understood based on the location of the associated halide ion relative to the excited-state dipole. For this class of chromophores, Blakley and Dearmond have shown that the charge-transfer dipole is directed toward the ligand that is most easily reduced. ⁴⁷ The first reduction potential of 1^{2+} is -880mV versus NHE, which compares favorably to that of the related [Ru(bpy-CONHEt)₃]^{2+*} (-880 mV vs NHE)⁴⁸ but not that of $[Ru(dtb)_3]^{2+}$ (-1000 mV vs NHE).⁴⁹ Therefore, in 1^{2+} , the excited-state dipole is directed toward the daea ligand, and the luminescent excited state was well formulated as [Ru^{III}(daea⁻)(dtb)₂]²⁺*, with the dipole directed toward the halide binding site. Hence, halide self-assembly in the excited state is formally described with an anionic ligand that destabilizes the excited state, resulting in a blue shift in PL.

In contrast, the electron-withdrawing groups in 2^{2+} lower the reduction potential to -470 mV, which compares reasonably with the -530 mV first reduction of $[Ru(btfmb)_3]^{2+}$. The excited state of 2^{2+} is hence well formulated as $[Ru^{III}(daea)-(btfmb^-)(btfmb)]^{2+}$. Hence, halide supramolecular assembly involves a ligand that is not directly aligned with the charge-transfer dipole that stabilizes the excited state, resulting in a red-shifted PL spectrum.

Pulsed-light excitation provided PL decays that were well described by a first-order kinetic model and yielded lifetimes of $\tau=1.18$ and $1.36~\mu s$ for 1^{2+} and 2^{2+} , respectively. Chloride titration studies with 1^{2+} led to the appearance of biexponential kinetics (Figures S12 and S13). At large chloride concentrations, a single-exponential decay was again recovered with $\tau=1.33~\mu s$. Quantum yield measurements performed in the absence and presence of excess chloride allowed the radiative and nonradiative rate constants for excited-state decay to be determined (Table 1). This analysis revealed that the increased

Table 1. Photophysical Properties of Complexes 1^{2+} , 2^{2+} , and Their Chloride Ion-Paired Analogues in CH_2Cl_2

	λ_{\max} (nm)					
	Abs	PL	τ (μs)	$\phi_{ ext{ iny PL}}$	$(\times 10^4 \text{ s}^{-1})$	$(\times 10^5 \mathrm{s}^{-1})$
12+	474	665	1.18	0.061	5.2	8.0
$[1^{2+},Cl^{-}]$	471	640	1.33	0.12	6.8	4.80
2^{2+}	459	600	1.36	0.095	7.0	6.7
$[2^{2+},Cl^{-}]$	469	630	1.78 ^a	b	ь	ь

^aEstimated from the time-resolved PL of 2²⁺ at 1 equiv of chloride. ^bUnable to be determined because of precipitation of the complex at high chloride concentrations.

lifetime and PL intensity associated with $\rm Cl^-$ assembly to $\rm 1^{2+}$ resulted from an approximately 2-fold change in the non-radiative rate constant. The analogous titration study with $\rm 2^{2+}$ was frustrated by precipitation and potential ligand substitution; however, no evidence for biexponential excited-state relaxation was observed.

The PL spectrum recorded at fixed delay times after pulsed-light excitation were measured and found to be very informative. Representative data are shown in Figure 3 for 1^{2+} and 2^{2+} with 1 equiv of chloride, abbreviated as $[1^{2+},Cl^-]^+$ and $[2^{2+},Cl^-]^+$, respectively. In the case of 1^{2+} , the PL spectrum measured 3 μ s after excitation was considerably red-shifted from that measured at a 45 ns delay time. Spectra recorded at intermediate times showed a continuous spectral shift to lower energy. These transient data are consistent with light excitation resulting in Cl^- release followed by reequilibration.

For 2^{2+} , the addition of chloride did not affect the timeresolved PL, which was well described by a first-order kinetic model throughout the titration. Transient PL experiments of 2^{2+} with 1 equiv of chloride did not show any time-dependent color change. It should be noted that the PL spectra measured in these transient experiments were different from the steady-state spectral data in Table 1 and Figure 2, which were corrected for the fluorimeter spectral response.

A square scheme with ground- and excited-state equilibria is proposed like those commonly used to understand photoacid/ base chemistry (Figure 4). $^{30,32-34,51}$ The ground-state equilibrium is associated with the excited-state equilibrium through light absorption to yield the thermally equilibrated photoluminescent excited state. The differential rate equations for the two excited-state species A* and B*, where A is either 1^{2+} or 2^{2+} and B is either 1^{2+} , CI^- or 1^{2+} , 1^{2-} , are given in eqs 1 and 2. The analytical solutions for these equations have been derived elsewhere 1^{32-34} and were used to fit the experimental data. An interesting point is that the rate constants extracted from a biexponential fit do not correspond to relaxation of the two excited states present (i.e., 1^{2+} , 1^{2+} , 1^{2+} , 1^{2+} , 1^{2+} , 1^{2+} , 1^{2+} , 1^{2+} , 1^{2+} , 1^{2+} , 1^{2+} , 1^{2+} , 1^{2+} , 1^{2+} , 1^{2+} , 1^{2+} , 1^{2+} , 1^{2+} , 1^{2+} , and were used to fit the experimental data. An interesting point is that the rate constants extracted from a biexponential fit do not correspond to relaxation of the two excited states present (i.e., 1^{2+}

$$\frac{d[A^*]}{dt} = -(k_{12} + k_1)[A^*] + k_{21}[B^*]$$
(1)

$$\frac{d[B^*]}{dt} = -(k_{21} + k_2)[B^*] + k_{12}[A^*]$$
(2)

Application of this kinetic analysis to 1^{2+*} gave the forward $(k_{12} = 1.8 \times 10^{11} \ \mathrm{M^{-1} \ s^{-1}})$ and reverse $(k_{21} = 9.1 \times 10^5 \ \mathrm{s^{-1}})$ rate constants that correspond to $K^*_{\mathrm{eq}} = 1.7 \times 10^5 \ \mathrm{M^{-1}}$, which differs from that of the ground state by a factor of 20 $(K_{\mathrm{eq}} = 3.9 \times 10^6 \ \mathrm{M^{-1}})$.

It should be emphasized that this analysis is for the thermally equilibrated excited state, and the rate constant for chloride dissociation in the initially formed Franck—Condon excited state may be much larger because relaxation back to the luminescent excited state occurs with the transfer of considerable electron density from the daea ligand back to the metal. The kinetic data are, nevertheless, important for understanding the behavior of the luminescent excited state. For example, 500 ns after photoexcitation of [1²⁺,Cl⁻]⁺, about 45% of the excited states have dissociated chloride (Figure S14).

Complex [2²⁺,CI⁻]⁺ displayed remarkably different excitedstate behavior than [1²⁺,CI⁻]⁺. In the time-resolved PL, the decay kinetics remained first-order even after the addition of chloride. Also, photoexcitation of the ion-paired complex did not result in time-dependent shifts in the PL spectra. Nonetheless, with regard to the red shift of the PL between 2²⁺ and [2²⁺,CI⁻]⁺, an increased equilbrium constant is expected. This was confirmed through Förster cycle analysis,

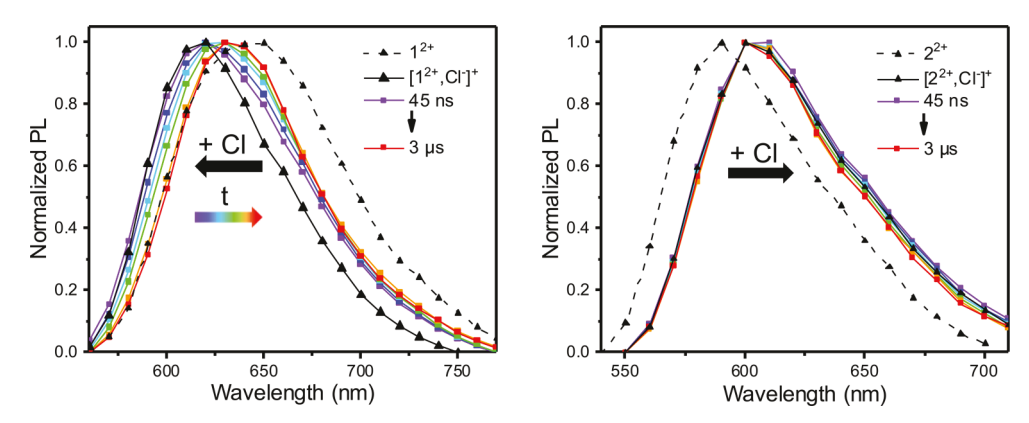


Figure 3. Transient PL spectra obtained at 45 ns (purple square) and at longer (purple to red) time delays after pulsed 500 nm laser excitation of 1^{2+} (left) and 2^{2+} (right) in the presence of 1 equiv of chloride. The PL spectra of the non-ion-paired complexes are also given for reference (black triangle, dashed line). The bold black arrow indicated the spectral shift expected for chloride self-assembly. The colored arrow indicates the time-dependent spectral shift.

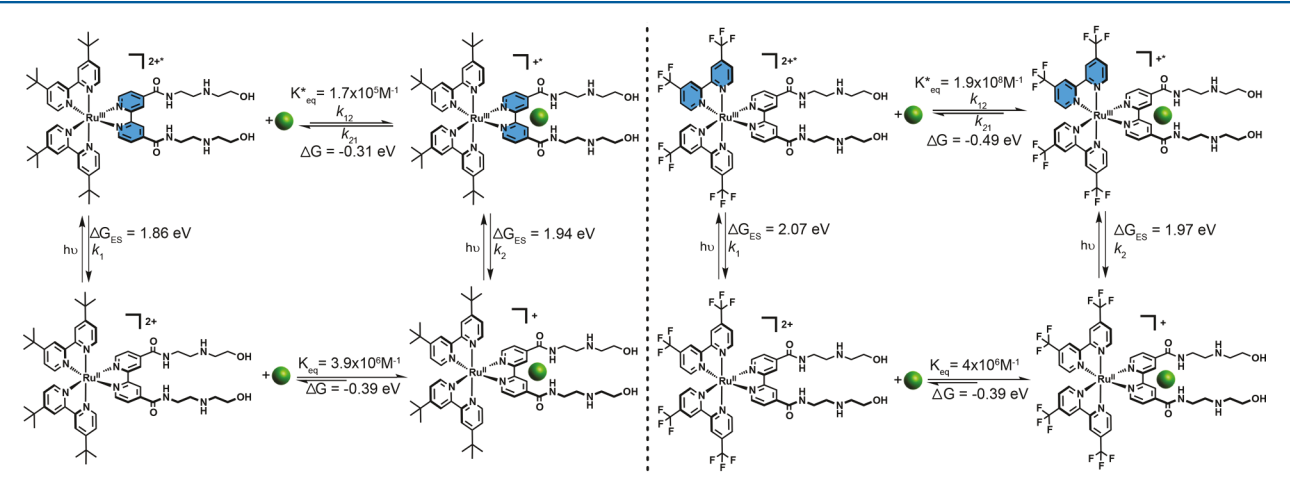


Figure 4. Square scheme for ground- and excited-state equilibria of 1^{2+} (left) and 2^{2+} (right) in the presence of chloride. The blue shading indicates the location of the electron in the MLCT excited state, while the green sphere represents chloride. Förster cycle analysis was used to calculate K^*_{eq} for 1^{2+} and 2^{2+} . The calculated K^*_{eq} for 1^{2+} is consistent with kinetic analysis from the square scheme.

which showed a 45-fold increase in the excited-state equilibrium constant (Table 2).

Table 2. Equilibrium Constants for 1²⁺ and 2²⁺ with Chloride in the Ground and Excited States

	$K_{ m eq}$	$K_{\rm eq}^*$	k_{12}	k_{21}
	(M^{-1})	(M^{-1})	$(\times 10^{11} \text{ M}^{-1} \text{ s}^{-1})$	$(\times 10^5 \text{ s}^{-1})$
[1 ²⁺ ,Cl ⁻] ⁺	3.9×10^{6}	1.7×10^{5}	1.8	9.1
[2 ²⁺ .Cl ⁻] ⁺	$4 \times 10^{6} a$	1.9×10^{8}	c	c

^aThe uncertainty was larger for this equilibrium because of precipitation of the complex at high chloride concentrations. ^bEstimated using a Förster cycle. ^cThere was no spectroscopic evidence for differing ground- and excited-state equilibria, precluding kinetic analysis.

The supramolecular assembly of chloride ions resulted in excited states that either retained, $[2^{2+}, CI^-]^{+*}$, or released, $[1^{2+}, CI^-]^{+*}$, chloride ions. The former are useful for chloride sensing, $^{1,2,12,13}_{1,2,12,13}$ while the latter may be exploited for delivery. The photorelease described here has the advantage of rapid release of CI^- in about 150 ns. The self-assembly of the photoreleased CI^- was advantageous for signal averaging with pulsed lasers but is not ideal for many other

applications. For biological and desalination applications, ^{26–28} halide self-assembly must occur in water, where irreversible release may be desired. The supramolecular assembly described here takes advantage of the Coulombic attraction of the dication chromophore and halide anion, as well as the hydrogen-bonding properties of the daea ligand. The low dielectric constant of the organic solvent utilized here enhances the Coulombic attraction, and for application in aqueous environments, the halide recognition ability of the ligand would require enhancement. The difference in the ground-and excited-state equilibrium constants, combined with advances in halide sensing in water, ¹ suggests that fine-tuning can be realized.

CONCLUSIONS

Two ruthenium chromophores, 1^{2+} and 2^{2+} , exhibited very different excited-state behaviors in the supramolecular assembly with chloride. When the excited-state dipole was directed away from the **daea** halide receptor ligand, as was the case for $[2^{2+},Cl^-]^+$, the equilibrium constant for chloride assembly in the excited state was greater than that in the ground state. In dramatic contrast, when the excited-state dipole was oriented toward the chloride anion, as was the case for $[1^{2+},Cl^-]^+$, the excited-state equilibrium constant was reduced by a factor of 20

from that of the ground state, which resulted in the rapid loss of the chloride ion upon light absorption. Preliminary results show that this approach is generalizable across the halide series, although excited-state reactivity was observed with iodide. However, such reactivity can be avoided through tuning of the excited-state reduction potentials.

Most practical applications of this advance would require aqueous conditions. The compounds presented herein are unlikely to even bind halides from water because halide binding is inversely proportional to the solvent dielectric constant. Indeed, about a 2 order of magnitude decrease in the equilibrium constant was found here when the solvent was changed from dichloromethane (ε = 8.9) to acetonitrile (ε = 37.5), which is in agreement with previous findings.⁴¹ Transposition to water ($\varepsilon = 80.1$) presents further challenges because favorable solvent-solute interactions must also be overcome.⁵⁸ However, significant advances in halide binding in water and organic solvent-water mixtures have been achieved through the use of rigid receptor ligands and supramolecular complexes such as cavitand, where the local polar environment is controlled at the molecular level. 58-60 Utilization of these supramolecular complexes with the correctly tuned excitedstate properties could one day lead to enhanced anion binding or photorelease in polar solvents. Overall, these data and analysis show that with appropriate synthetic design, chromophores that rapidly release or completely retain a chloride ion when excited with visible light can be realized in a fluid solution.

ASSOCIATED CONTENT

S Supporting Information

The Supporting Information is available free of charge on the ACS Publications website at DOI: 10.1021/acs.inorg-chem.8b00559.

Characterization for newly reported compounds, ¹H NMR titration, time-resolved PL decay, electrochemistry, and UV—vis titration (PDF)

AUTHOR INFORMATION

Corresponding Author

*E-mail: gjmeyer@email.unc.edu.

ORCID

Ludovic Troian-Gautier: 0000-0002-7690-1361 Renato N. Sampaio: 0000-0002-7158-6470 Gerald J. Meyer: 0000-0002-4227-6393

Notes

The authors declare no competing financial interest.

ACKNOWLEDGMENTS

We acknowledge support from the National Science Foundation (Award CHE-1213357). M.D.T. acknowledges support from the Nation Science Foundation Graduate Research Fellowship Program under Grant DGE-1650116. L.T.-G. acknowledges the Belgian American Educational Foundation as well as the Bourse d'Excellence Wallonie-Bruxelles (WBI.World) for generous support. The authors thank the Core Laboratory, Department of Chemistry Mass Spectrometry, University of North Carolina, and Dr. B. Ehrmann for assistance with mass spectrometry analysis.

■ REFERENCES

- (1) Beer, P. D.; Gale, P. A. Anion Recognition and Sensing: The State of the Art and Future Perspectives. *Angew. Chem., Int. Ed.* **2001**, 40, 486–516.
- (2) Evans, N. H.; Beer, P. D. Advances in Anion Supramolecular Chemistry: From Recognition to Chemical Applications. *Angew. Chem., Int. Ed.* **2014**, *53*, 11716–11754.
- (3) Liu, Y.; Sengupta, A.; Raghavachari, K.; Flood, A. H. Anion Binding in Solution: Beyond the Electrostatic Regime. *Chem.* **2017**, *3*, 411–427.
- (4) Rebarz, M.; Marcélis, L.; Menand, M.; Cornut, D.; Moucheron, C.; Jabin, I.; Kirsch-De Mesmaeker, A. Revisited Photophysics and Photochemistry of a Ru-TAP Complex Using Chloride Ions and a Calix[6]crypturea. *Inorg. Chem.* **2014**, 53, 2635–2644.
- (5) Brunetti, E.; Picron, J. F.; Flidrova, K.; Bruylants, G.; Bartik, K.; Jabin, I. Fluorescent Chemosensors for Anions and Contact Ion Pairs with a Cavity-Based Selectivity. *J. Org. Chem.* **2014**, *79*, 6179–6188.
- (6) Goursaud, M.; De Bernardin, P.; Dalla Cort, A.; Bartik, K.; Bruylants, G. Monitoring Fluoride Binding in DMSO: Why is a Singular Binding Behavior Observed? *Eur. J. Org. Chem.* **2012**, 2012, 3570–3574.
- (7) Lau, Y. H.; Rutledge, P. J.; Watkinson, M.; Todd, M. H. Chemical sensors that incorporate click-derived triazoles. *Chem. Soc. Rev.* **2011**, 40, 2848–2866.
- (8) Dalla Cort, A.; De Bernardin, P.; Forte, G.; Yafteh Mihan, F. Metal-Salophen-Based Receptors for Anions. *Chem. Soc. Rev.* **2010**, 39, 3863–3874.
- (9) Cametti, M.; Rissanen, K. Recognition and sensing of fluoride anion. *Chem. Commun.* **2009**, 2809–2829.
- (10) Cametti, M.; Dalla Cort, A.; Bartik, K. Fluoride Binding in Water: A New Environment for a Known Receptor. *ChemPhysChem* **2008**, *9*, 2168–2171.
- (11) Bisson, A. P.; Lynch, V. M.; Monahan, M. K. C.; Anslyn, E. V. Recognition of Anions through NH- π Hydrogen Bonds in a Bicyclic Cyclophane- Selectivity for Nitrate. *Angew. Chem., Int. Ed. Engl.* **1997**, 36, 2340–2342.
- (12) Szemes, F.; Hesek, D.; Chen, Z.; Dent, S. W.; Drew, M. G. B.; Goulden, A. J.; Graydon, A. R.; Grieve, A.; Mortimer, R. J.; Wear, T.; Weightman, J. S.; Beer, P. D. Synthesis and Characterization of Novel Acyclic, Macrocyclic, and Calix[4]arene Ruthenium(II) Bipyridyl Receptor Molecules That Recognize and Sense Anions. *Inorg. Chem.* 1996, 35, 5868–5879.
- (13) Uppadine, L. H.; Drew, M. G. B.; Beer, P. D. Anion Selectivity Properties of Ruthenium(II) tris(5,5'-diamide-2,2'-bipyridine) Receptors Dictated by Solvent and Amide Substituent. *Chem. Commun.* **2001**, 291–292.
- (14) Glebov, E. M.; Pozdnyakov, I. P.; Plyusnin, V. F.; Khmelinskii, I. Primary Reactions in the Photochemistry of Hexahalide Complexes of Platinum Group Metals: A Minireview. *J. Photochem. Photobiol., C* **2015**, *24*, 1–15.
- (15) Balzani, V.; Manfrin, F.; Moggi, L. Photochemistry of Coordination Compounds. XVI. Hexabromoplatinate(IV) and Hexaiodoplatinate(IV) Ions. *Inorg. Chem.* **1967**, *6*, 354–358.
- (16) Balzani, V.; Carassiti, V. Photochemistry of Some Square-Planar and Octahedral Platinum Complexes. *J. Phys. Chem.* **1968**, 72, 383–388.
- (17) Pozdnyakov, I. P.; Glebov, E. M.; Plyusnin, V. F.; Tkachenko, N. V.; Lemmetyinen, H. Primary Processes in Photophysics and Photochemistry of PtBr₆²⁻ Complex Studied by Femtosecond Pump–Probe Spectroscopy. *Chem. Phys. Lett.* **2007**, 442, 78–83.
- (18) Glebov, E. M.; Plyusnin, V. F.; Grivin, V. P.; Venediktov, A. B.; Korenev, S. V. Photochemistry of ${\rm PtBr_6}^{2-}$ in Aqueous Solution. *Russ. Chem. Bull.* **2007**, *56*, 2357–2363.
- (19) Wright, R. C.; Laurence, G. S. Production of Platinum(III) by Flash Photolysis of ${\rm PtCl_6}^2$. *J. Chem. Soc., Chem. Commun.* **1972**, 132–133.
- (20) Znakovskaya, I. V.; Sosedova, Y. A.; Glebov, E. M.; Grivin, V. P.; Plyusnin, V. F. Intermediates Formed by Laser Flash Photolysis of

 $[PtCl_6]^{2-}$ in Aqueous Solutions. *Photochem. Photobiol. Sci.* **2005**, 4, 897–902.

- (21) Wong, C. F. C.; Kirk, A. D. Chloride Quantum Yields from Photolysis of Chloropentammine and Chloropentakisalkynlamino Chromium(III) Complexes. *Can. J. Chem.* 1974, 52, 3384–3386.
- (22) Adamson, A. W. Photochemistry of Complex Ions. The Role of Quartet Excited States in the Photochemistry of Chromium (III) Complexes. *J. Phys. Chem.* **1967**, *71*, 798–808.
- (23) Kirk, A. D.; Moss, K. C.; Valentin, J. G. Photochemistry of the cis- and trans-Dichlorobisethylenediamine Chromium(III) Cations in Acidic Solutions. Observation of a Stereochemical Change in Photoaquation. Can. J. Chem. 1971, 49, 1524–1528.
- (24) Sheridan, P. S.; Adamson, A. W. Photochemistry of Complex Ions. cis- $[Co(en)_2Cl_2]^+$ and $_{cis}$ - $[Co(en)_2(H_2O)Cl]^{2+}$. J. Am. Chem. Soc. 1974, 96, 3032–3038.
- (25) Pribush, R. A.; Poon, C. K.; Bruce, C. M.; Adamson, A. W. Photochemistry of Complex Ions. Photochemistry of Cobalt(III) Acidoammines. J. Am. Chem. Soc. 1974, 96, 3027–3032.
- (26) Werber, J. R.; Osuji, C. O.; Elimelech, M. Erratum: Materials for Next-Generation Desalination and Water Purification Membranes. *Nat. Rev. Mater.* **2016**, *1*, 1–15.
- (27) White, W.; Sanborn, C. D.; Reiter, R. S.; Fabian, D. M.; Ardo, S. Observation of Photovoltaic Action from Photoacid-Modified Nafion Due to Light-Driven Ion Transport. *J. Am. Chem. Soc.* **2017**, *139*, 11726–11733.
- (28) Cutting, G. R. Cystic fibrosis genetics: from molecular understanding to clinical application. *Nat. Rev. Genet.* **2015**, *16*, 45–56.
- (29) Hadda, T. B.; Le Bozec, H. Preparation and Characterization of Ruthenium Complexes with the New 4,4',4"-tri-tert-butylterpyridine Ligand and with 4,4'-di-tert-butylbipyridine. *Polyhedron* **1988**, 7, 575–577.
- (30) O'Donnell, R. M.; Sampaio, R. N.; Li, G.; Johansson, P. G.; Ward, C. L.; Meyer, G. J. Photoacidic and Photobasic Behavior of Transition Metal Compounds with Carboxylic Acid Group(s). *J. Am. Chem. Soc.* **2016**, *138*, 3891–3903.
- (31) Crosby, G. A.; Demas, J. N. The Measurement of Photoluminescence Quantum Yields. A Review. *J. Phys. Chem.* **1971**, *75*, 991–1024.
- (32) Loken, M. R.; Hayes, J. W.; Gohlke, J. R.; Brand, L. Excited-State Proton Transfer as a Biological Probe. Determination of Rate Constants by Means of Nanosecond Fluorometry. *Biochemistry* **1972**, *11*, 4779–4786.
- (33) Demas, J. N. In Excited State Lifetime Measurements; Demas, J. N., Ed.; Academic Press: New York, 1983; p 43.
- (34) Laws, W. R.; Brand, L. Analysis of Two-State Excited-State Reactions. The Fluorescence Decay of 2-Naphthol. *J. Phys. Chem.* **1979**, 83, 795–802.
- (35) Connelly, N. G.; Geiger, W. E. Chemical Redox Agents for Organometallic Chemistry. *Chem. Rev.* **1996**, *96*, 877–910.
- (36) Noviandri, I.; Brown, K. N.; Fleming, D. S.; Gulyas, P. T.; Lay, P. A.; Masters, A. F.; Phillips, L. The Decamethylferrocenium/Decamethylferrocene Redox Couple: A Superior Redox Standard to the Ferrocenium/Ferrocene Redox Couple for Studying Solvent Effects on the Thermodynamics of Electron Transfer. *J. Phys. Chem. B* 1999, 103, 6713–6722.
- (37) Lin, S.; Ischay, M. A.; Fry, C. G.; Yoon, T. P. Radical Cation Diels-Alder Cycloadditions by Visible Light Photocatalysis. *J. Am. Chem. Soc.* **2011**, *133*, 19350–19353.
- (38) Ischay, M. A.; Ament, M. S.; Yoon, T. P. Crossed intermolecular [2 + 2] cycloaddition of styrenes by visible light photocatalysis. *Chem. Sci.* **2012**, *3*, 2807–2811.
- (39) Fielding, L. Determination of Association Constants (K_a) from Solution NMR Data. *Tetrahedron* **2000**, *56*, 6151–6170.
- (40) Ward, W. M.; Farnum, B. H.; Siegler, M.; Meyer, G. J. Chloride Ion-Pairing with Ru(II) Polypyridyl Compounds in Dichloromethane. *J. Phys. Chem. A* **2013**, *117*, 8883–8894.
- (41) Troian-Gautier, L.; Beauvilliers, E. E.; Swords, W. B.; Meyer, G. J. Redox Active Ion-Paired Excited States Undergo Dynamic Electron Transfer. J. Am. Chem. Soc. 2016, 138, 16815–16826.

- (42) Swords, W. B.; Li, G.; Meyer, G. J. Iodide Ion Pairing with Highly Charged Ruthenium Polypyridyl Cations in CH₃CN. *Inorg. Chem.* **2015**, *54*, 4512–4519.
- (43) Wehlin, S. A. M.; Troian-Gautier, L.; Li, G.; Meyer, G. J. Chloride Oxidation by Ruthenium Excited-states in Solution. *J. Am. Chem. Soc.* **2017**, *139*, 12903–12906.
- (44) Benesi, H. A.; Hildebrand, J. H. A Spectrophotometric Investigation of the Interaction of Iodine with Aromatic Hydrocarbons. J. Am. Chem. Soc. 1949, 71, 2703–2707.
- (45) Gu, J.; Yan, Y.; Helbig, B. J.; Huang, Z.; Lian, T.; Schmehl, R. H. The Influence of Ligand Localized Excited States on the Photophysics of Second Row and Third Row Transition Metal Terpyridyl Complexes: Recent Examples and a Case Study. *Coord. Chem. Rev.* 2015, 282–283, 100–109.
- (46) Li, G.; Brady, M. D.; Meyer, G. J. Visible Light Driven Bromide Oxidation and Ligand Substitution Photochemistry of a Ru Diimine Complex. *J. Am. Chem. Soc.* **2018**, *140*, 5447–5456, DOI: 10.1021/jacs.8b00944.
- (47) Blakley, R. L.; Dearmond, M. K. Unique Spectroscopic Properties of Mixed-Ligand Complexes with 2,2'-Dipyridylamine: A Dual Luminescence from a Ruthenium(II) Complex. *J. Am. Chem. Soc.* 1987, 109, 4895–4901.
- (48) Elliott, C. M.; Hershenhart, E. J. Electrochemical and Spectral Investigations of Ring-Substituted Bipyridine Complexes of Ruthenium. *J. Am. Chem. Soc.* **1982**, *104*, 7519–7526.
- (49) Rota Martir, D.; Averardi, M.; Escudero, D.; Jacquemin, D.; Zysman-Colman, E. Photoinduced Electron Transfer in Supramolecular Ruthenium—Porphyrin Sssemblies. *Dalton Trans.* **2017**, 46, 2255–2262.
- (50) Jang, H. J.; Hopkins, S. L.; Siegler, M. A.; Bonnet, S. Frontier Orbitals of Photosubstitutionally Active Ruthenium Complexes: An Experimental Study of the Spectator Ligands' Electronic Properties Influence on Photoreactivity. *Dalton Trans.* **2017**, *46*, 9969–9980.
- (51) Ireland, J. F.; Wyatt, P. A. H. In *Advances in Physical Organic Chemistry*; Gold, V., Ed.; Academic Press: New York, 1976; Vol. 12, p 131.
- (52) Zhou, D.; Khatmullin, R.; Walpita, J.; Miller, N. A.; Luk, H. L.; Vyas, S.; Hadad, C. M.; Glusac, K. D. Mechanistic Study of the Photochemical Hydroxide Ion Release from 9-Hydroxy-10-methyl-9-phenyl-9,10-dihydroacridine. *J. Am. Chem. Soc.* **2012**, *134*, 11301–11303.
- (53) Xie, Y.; Ilic, S.; Skaro, S.; Maslak, V.; Glusac, K. D. Excited-State Hydroxide Ion Release From a Series of Acridinol Photobases. *J. Phys. Chem. A* **2017**, *121*, 448–457.
- (54) Hidayatullah, A. N.; Wachter, E.; Heidary, D. K.; Parkin, S.; Glazer, E. C. Photoactive Ru(II) Complexes With Dioxinophenanthroline Ligands Are Potent Cytotoxic Agents. *Inorg. Chem.* **2014**, *53*, 10030–10032.
- (55) Wachter, E.; Glazer, E. C. Mechanistic Study on the Photochemical "Light Switch" Behavior of $[Ru(bpy)_2dmdppz]^{2+}$. *J. Phys. Chem. A* **2014**, *118*, 10474–10486.
- (56) Kohler, L.; Nease, L.; Vo, P.; Garofolo, J.; Heidary, D. K.; Thummel, R. P.; Glazer, E. C. Photochemical and Photobiological Activity of Ru(II) Homoleptic and Heteroleptic Complexes Containing Methylated Bipyridyl-type Ligands. *Inorg. Chem.* **2017**, *56*, 12214–12223.
- (57) Qu, F.; Park, S.; Martinez, K.; Gray, J. L.; Thowfeik, F. S.; Lundeen, J. A.; Kuhn, A. E.; Charboneau, D. J.; Gerlach, D. L.; Lockart, M. M.; Law, J. A.; Jernigan, K. L.; Chambers, N.; Zeller, M.; Piro, N. A.; Kassel, W. S.; Schmehl, R. H.; Paul, J. J.; Merino, E. J.; Kim, Y.; Papish, E. T. Ruthenium Complexes are pH-Activated Metallo Prodrugs (pHAMPs) with Light-Triggered Selective Toxicity Toward Cancer Cells. *Inorg. Chem.* **2017**, *56*, 7519–7532.
- (58) Kubik, S. Anion Recognition in Water. *Chem. Soc. Rev.* **2010**, *39*, 3648–3663.
- (59) Langton, M. J.; Serpell, C. J.; Beer, P. D. Anion Recognition in Water: Recent Advances from a Supramolecular and Macromolecular Perspective. *Angew. Chem., Int. Ed.* **2016**, *55*, 1974–1987.

(60) Wenzel, M.; Weigand, J. J. Recent Advances in Anion Recognition. *J. Inclusion Phenom. Macrocyclic Chem.* **2017**, 89, 247–251.